Freeze-Fracture and Electrophysiological Studies of Newly Developed Acetylcholine Receptors in *Xenopus* Embryonic Muscle Cells

P. C. BRIDGMAN, S. NAKAJIMA, A. S. GREENBERG, and Y. NAKAJIMA

Department of Biological Sciences, Purdue University, West Lafayette, Indiana 47907. Dr. Bridgman's present address is Laboratory of Neurobiology, National Institute of Neurological and Communicative Disorders and Stroke, National Institutes of Health, Bethesda, Maryland 20205; Dr. Greenberg's present address is Department of Neurobiology and Behavior, State University of New York, Stony Brook, New York 11794.

ABSTRACT The development of acetylcholine receptors on *Xenopus* embryonic muscle cells both in culture and in situ was studied using electrophysiology and freeze-fracture electron microscopy. Acetylcholine sensitivity first appeared at developmental stage 20 and gradually increased up to about stage 31. Freeze-fracture of muscle cells that were nonsensitive to acetylcholine revealed diffusely distributed small P-face intramembraneous particles. When cells acquired sensitivity to acetylcholine, a different group of diffusely distributed large P-face particles began to appear. This group of particles was analyzed by subtracting the size distribution found on nonsensitive cells from that found on sensitive cells. We call this group of particles difference particles. The sizes of difference particles were large (peak diameter 11 nm). The density of difference particles gradually increased with development. The density of small particles (<9 nm) did not change with development. At later stages (32–36) aggregates of large particles appeared, which probably represent acetylcholine receptor clusters. The size distribution of difference particles was close to that of the aggregated particles, suggesting that at least part of difference particles represent diffusely distributed acetylcholine receptors. Difference particles exist mostly in solitary form (occasionally double), indicating that an acetylcholine receptor can be functional in solitary form. This result also shows that diffuse acetylcholine receptors that have previously been observed with ^{125}I-α-bungarotoxin autoradiography do indeed exist in solitary forms not as microaggregates.

During embryonic development acetylcholine (ACh)[1] receptors begin to emerge on the surface membrane of embryonic muscle cells before innervation takes place (4). At this early stage of development, ACh receptors, as revealed by autoradiography of α-bungarotoxin binding sites, appear to be distributed diffusely over the surface membrane. Upon innervation ACh receptors begin to be localized. The time taken for the localization varies among animals, but eventually almost all ACh receptors are clustered together at neuromuscular junctions. This kind of developmental sequence occurs in cultured materials as well as during natural development (1, 3, 10, 13, 15, 16–18, 21, 26, 34, 48, 49, 52).

[1] *Abbreviation used in this paper:* ACh, acetylcholine.

The ultrastructure of clustered ACh receptors has been extensively studied electron microscopically through freeze-fracture, deep-etching, or negative-staining techniques. These studies have shown that clustered ACh receptors appear as aggregates of large particles, and it is likely that each particle (which may consist of five subunits) represents a single ACh receptor molecule (11, 12, 22, 23, 40, 43–45, 47, 53). The structure of diffusely distributed ACh receptors, however, has not been studied, primarily because of the difficulty in identifying nonclustered receptors. The main objective of the present study is to elucidate the ultrastructure of these diffusely distributed ACh receptors at early stages of development. Another aim of the present investigation is to observe how the function of ACh receptors and the membrane struc-

THE JOURNAL OF CELL BIOLOGY · VOLUME 98 JUNE 1984 2160–2173

ture change during early stages of development starting just after their first insertion in the membrane. Although, Hartzell and Fambrough (21) conducted experiments to determine the development of ACh receptors, they did not deal with these early stages. In addition, they used autoradiography to observe α-bungarotoxin binding sites, whereas our methods for detecting ACh receptors, are freeze-fracture and electrophysiology.

Specific questions we wished to answer were these: Do newly developed functional ACh receptors, which appear to be distributed diffusely when seen in autoradiography, exist as solitary particles when seen with freeze-fracture electron microscopy, or do they exist in small aggregates scattered over the surface? Are there differences in the size of these newly developed receptors when compared with the aggregated ACh receptor of later stages? Is there a physiologically inactive form of ACh receptor at an initial stage? We have tried to answer these questions by correlating physiological data with structural findings. We have used embryonic *Xenopus* muscle cells. These cells were the most convenient materials for our purpose: it is known that their development takes place very rapidly and that at a certain critical time the cells start to acquire sensitivity to externally applied acetylcholine (4). Muscle cells in culture allowed us to perform critical experiments that were not feasible with embryonic cells in situ. One of the main conclusions of the present study is that ACh receptors at early stages are seen as diffusely distributed large intramembrane particles, which exist in singular form (occasionally double) not as microaggregates. This suggests that a solitary ACh receptor molecule can function independently of other ACh receptors. Part of the results have been reported at a few meetings (7–9).

MATERIALS AND METHODS

The main experiments were performed using muscle cells in culture (without neural tissue) derived from *Xenopus* embryos. The usual procedures were first to measure the sensitivity to ACh through electrophysiological techniques, and then to use the same cell for ultrastructural studies by means of freeze-fracture electron microscopy. In another series of experiments, we used *Xenopus* embryonic muscle cells in situ. In this case, however, it was impossible to correlate electrophysiology with morphology quantitatively.

Preparation of Xenopus Embryos and Muscle Cultures: *Xenopus* embryos were prepared as described previously (43, 44). The embryos were allowed to develop in 10% Holtfreter solution (Table I). The speed of development was controlled by adjusting the ambient temperature within 16–22°C.

For tissue culture we used a slightly different procedure than that described by Peng and Nakajima (43). Myotome cells were dissected from stage 14–16 embryos (41). These stages are well before ACh receptors emerge or innervation takes place (4, 31). Thus, we can regard our myotome cells as free from direct neuronal influences. The embryos were bisected with a small piece of razor blade into dorsal and ventral halves. The dorsal portion was treated for ~30 min with 1 mg/ml collagenase dissolved in Steinberg's solution (Table I). The myotomes were then teased away from the adjoining tissue with sharp needles, and the cells were dissociated in Ca^{++}-free, Mg^{++}-free Steinberg's solution containing 0.4 mM EGTA. Dissociation of the cells occurred in 30–60 min. The cells were plated onto 4-mm diam glass disks (cut from No. 0 or No. 1 coverglass) that were immersed in culture medium (Table I) in plastic culture dishes. The cultures were maintained at room temperature (23–24°C).

Electrophysiology on Cultured Muscle Cells: The cultured myotome cells grown on the glass disks were transfered from the culture dish to a recording chamber. The bathing solution was switched to a calcium-rich (10 mM) Steinberg's solution (Table I). The cells were viewed under a phase-contrast microscope with a water immersion objective (Carl Zeiss, Inc., New York; × 40; numerical aperture 0.75). Some cells were in close contact with each other, and others were isolated. We used only isolated cells for our experiments. The membrane potential was recorded through an intracellular microelectrode (3 M KCl, 70–120 MΩ). The input resistance of cultured myotome cells is very large (up to 2.6 giga-Ω). Therefore, the input amplifier stage must have a large input impedance and a very small input bias current. In order to record potential and pass current through the same electrode, an active bridge circuit, based on the principle used by Ito (25) and Takahashi (50), was designed (Fig. 1). The head stage was a Picometric Amplifier (Instrumentation Laboratory, Inc., Lexington, MA), which had an extremely small bias current (10^{-13}A). The current was measured through amplifier 4, as a voltage drop through the resistor ($10^{9}\Omega$) at the input. The equivalent input impedance of the bridge circuit was ~20 giga-Ω.

ACh sensitivity was measured by recording membrane potential changes produced by iontophoretic application of ACh (14, 17, 27, 30). The pipettes were filled with 2 M ACh chloride and had resistances of 100–200 MΩ. The level of braking current (1.5–3.0 nA) for the prevention of ACh leakage from the pipette was determined with a procedure similar to the one used for Kuffler and Yoshikami (30). The ACh sensitivity was measured from the maximum slope of the curve relating the electrical charge applied and the magnitude of depolarization (ACh depolarization). All experiments were performed at room temperature 23–24°C.

Additional Experiments: The methods so far described generally pertain to the main experiments conducted from 1979 to 1980. Recently (1982–1983), we obtained more electrophysiological data on cultured cells (shown in Fig. 5*B*). In these latter experiments, we made several minor modifications of the experimental procedures. The cultured cells were grown in culture dishes without glass disks. The temperatures at early stages (up to about stage 25) were maintained at slightly lower temperatures (18–20°C) to slow down the development: this made the experiments at early stages less hectic (the experiment itself was always done at room temperature). After stage 25, the culture dishes were maintained at room temperature. The intracellular electrode was filled with 4 M K acetate, instead of KCl. rather than determining an appropriate braking current for the ACh electrode before each experiment, we tried to maintain the braking currents constant: in almost all the cells the braking currents were between 2.0 and 4.2 nA. Nonetheless, we later realized that a small variation of braking current has a fairly large effect on the sensitivity if it exceeded 3.0 nA. Thus, we investigated the effect of braking current on the ACh sensitivity in nine cells (with seven different electrodes). The results showed, for example, that the sensitivity decreased by 30% when the braking current was increased from 3.0 to 4.0 nA. These data allowed us to correct the sensitivity for the variation of the braking current for each experiment.

Input Resistance of Cells in Culture: The muscle cell input resistance was measured through the bridge circuit. In the 1979–1980 experiments, in which both physiological and freeze-fracture data were obtained in the same cells (data in Fig. 5*A*), 38 cells out of the total of 51 had a membrane time constant >8 ms; in these cells it was not difficult to balance the bridge circuit by visual inspection (cf., Kidokoro et al. [27]). In 8 out of the 12 cells that had a time constant <8 ms, the visually balanced electrotonic potential coincided with that determined by an extrapolation procedure on semilogarithmic plot within 10% error (the extrapolation to zero time was made based on the assumption that the recorded response was composed of two parts: one

TABLE I

Concentration of the Solutions

	NaCl	KCl	$Ca(NO_3)_2$	$MgSO_4$	$CaCl_2$	$NaHCO_3$	HEPES-NaOH (pH 7.4)
				mM			
Steinberg	58	0.67	0.34	0.83	—	—	10
Holtfreter	60	0.67	—	—	0.68	0.59	—
Ringer	120	2.5	—	—	10	—	3.0
Ca^{++}-rich Steinberg	58	0.67	0.34	0.83	10	—	10

Culture medium: 88% Steinberg's solution, 10% L-15, 1% fetal bovine serum, 1% of penicillin-streptomycin solution containing 10,000 U penicillin/ml and 10,000 μg streptomycin/ml.

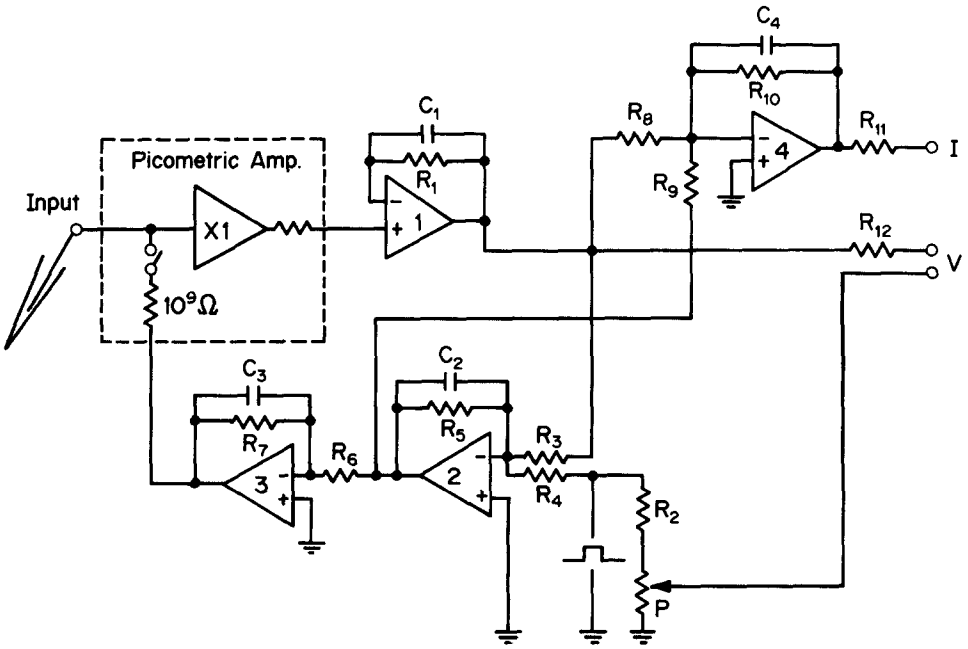

FIGURE 1 Active bridge circuit for recording membrane potential and passing current used for cultured cells. The head stage is a picometric amplifier (Instrumentation Laboratory, Inc., Lexington, MA). The overall gain from the input of the picometer amplifier to the output of the amplifier 1 stage is adjusted to exactly 1. The gain of amplifier 3 stage is also adjusted to exactly 1. The gain of amplifier 2 stage was ~0.95. The amplifier 4 stage measures the current as a voltage drop across 10^9 Ω. Amplifiers 1, 2, 3, 4 = Philbrick 1011 (Teledyne-Philbrick, Dedham, MA). Approximate values of the components are R_1, R_3, R_5, R_6, R_7 = 1,000 Ω. R_8,, R_9, R_{10} = 10,000 Ω. R_4 = 100,000 Ω. R_2 = 47,000 Ω. R_{11}, R_{12}, = 47 Ω. P = 10,000 Ω. C_1, C_2, C_3, C_4 = 25 pico-farads (pF).

from a fast stray-capacity transient, the other membrane potential transient.) In these cells, even if the time constants were <8 ms, visual balancing would have given a fairly good estimate of membrane resistance. In the rest of the cells (four cells) the resistance estimate could have been rather inaccurate, and in one cell the resistance was estimated from the cell size. In spite of this uncertainty, all the data are included in Fig. 5*A* because this group of cells (total 51) were also used for freeze-fracture electron microscopy (shown in Fig. 9).

Partly because of this uncertainty about the data of Fig. 5*A*, we repeated experiments in 1982–1983, and the data are shown in Fig. 5*B*. All the data in Fig. 5*B* were obtained from cells having the time constant >10 ms.

Electrophysiology on Xenopus Muscles In Situ: The purpose of the electrophysiological experiments in situ was to determine whether the myotome cells of different stage embryos had sensitivity to bath-applied ACh before being freeze-fractured. The embryo was pinned down on a Sylgard-lined (Dow Corning Corp., Midland, MI) recording chamber (vol 1 ml), and was continuously superfused with frog Ringer's solution (Table I). Under a stereomicroscope the ectoderm overlying the myotomes was teased away with a needle. Myotome cells in anteriorly located somites were impaled with a conventional intracellular microelectrode. Cells with a resting potential more negative than −60 mV were tested for ACh sensitivity by introducing one to a few drops of 10^{-4} g/ml ACh chloride into the perfusion system. The mouth of the perfusion tubing was very close to the myotome (within 2 mm).

The presence of ACh sensitivity was indicated by a depolarization that was initiated by the ACh introduction. The depolarization returned to the base line within 10–20 s (Fig. 11) due to desensitization and/or to washing away of the ACh by the superfusion. With this method the concentration of ACh applied to the cell is not known. However, it must have been more than enough to detect sensitivity, because ACh responses were always elicited, without exception, in the cells from which spontaneous endplate potentials were recorded.

Freeze-Fracture Electronmicroscopy: After electrophysiological recording from a cultured cell, it was photographed for later identification and fixed with 0.5% glutaraldehyde plus 5 mM $CaCl_2$ in 0.05 M Na cacodylate buffer (pH 7.1) for 1 h. The specimen was washed three times with buffer and equilibrated with 20% glycerol in buffer at room temperature for 30–60 min. Whole embryos were fixed with 2% glutaraldehyde plus 10 mM $CaCl_2$ in 0.1 M Na cacodylate buffer (pH 7.1) for 1–2 h. After equilibration with 20% glycerol in buffer at room temperature, the somite to be fractured was dissected free. Freeze-fracture procedures with the double replica device by means of the gold disk-coverglass sandwich technique have been described previously (43, 44, 53). Electron micrographs of the replicas were taken with a Philips EM 300 (Philips Electronic Instruments, Inc., Mahway, NJ).

Particle Size Analysis: High-magnification photographs of the freeze-fracture replicas were taken from the P face of the fractured membrane leaflet in three different areas of the cell. The final magnification of each photograph (× 384,000) was calibrated by means of a waffle calibration grid (Ladd Research Industries, Inc., Burlington, VT). The maximum widths of particle shadows were measured perpendicular to the shadowing direction by using a Hewlett-Packard digitizer and desk-top computer (Hewlett-Packard Co., Palo Alto, CA). All particles from the three areas were measured. The number of particles measured per cell ranged from 600 to 1,400.

Solutions: Compositions of the solutions are listed in Table I.

RESULTS

Data on cultured cells will be described first, followed by results on muscle cells in situ.

Corresponding Stage of Cultured Cells

When expressing developmental stage in culture, it is customary to state the stage in terms of the time after the culture is started (19, 27). However, it is desirable to compare the results on cultured cells with those on embryonic cells in situ. Thus, we shall express the developmental stage of cultured cells in terms of the corresponding stage. The corresponding stage was determined from observing the developmental stage (41) of normally developing embryos that originated from the same batch of eggs as used for the culture. These embryos, which served as a "calibrator" for determining the stages of the cultured cells, were kept near the tissue culture dishes at room temperature (23–24°C). All embryos from a single batch of eggs went through each developmental stage almost synchronously, inasmuch as the eggs were artificially inseminated at the same time.

Fig. 2 *A–E* shows phase-contrast microscopic pictures of typical muscle cells in culture at various corresponding stages. In early stages of culture most muscle cells assumed a characteristic bipolar spindle form as shown in Fig. 2. Occasionally tripolar or more complex forms were also seen. Under the phase-contrast microscope these muscle cells always appeared bright, with high contrast against the background, probably because the cells are thick. On the other hand, fibroblasts or other contaminating cell types, which were rarely encountered, usually spread in a circular or semicircular form, and were thin and more difficult to distinguish from the background. There was, thus, little danger of confusing the different cell types. To insure that we were testing only muscle cells, we impaled only bipolar spindle shaped cells during the early stages of development. In Fig. 2*F* the developmental stages of embryos and the length of time after plating (stage 18) are compared, the data being taken from Nieuwkoop and

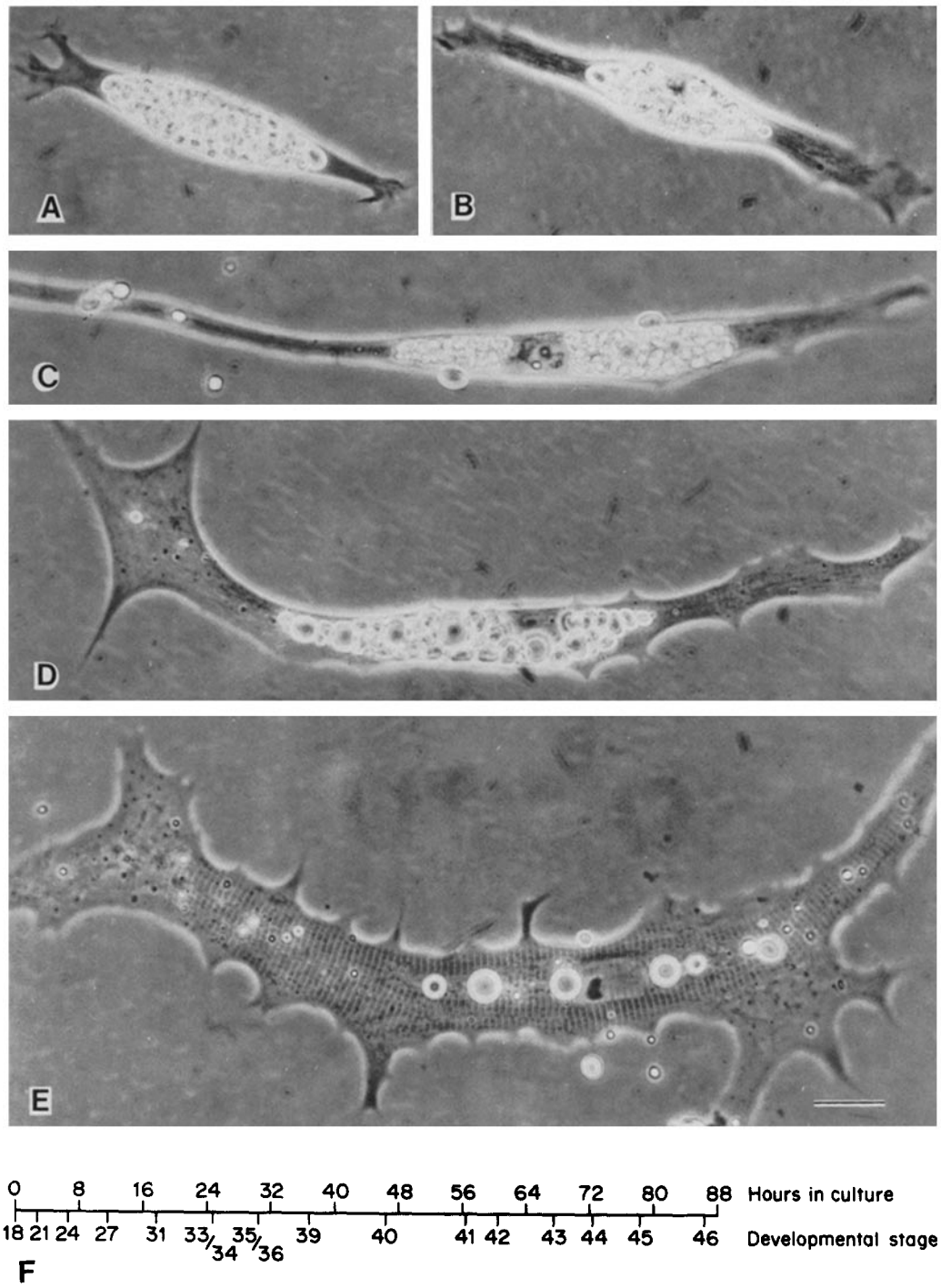

FIGURE 2 *A–E* Phase-contrast photomicrographs of *Xenopus* embryonic cells in culture. The myotomes were dissected at stage 14. (*A*) Stage 22; (*B*) stage 24; (*C*) stage 26; (*D*) stage 35/36; (*E*) stage 46. The calibration mark refers to 20 μm. (*F*) The length of time in culture is compared with the developmental stages for normally growing embryos at 22–24°C. Zero time refers to the point at which the cells were plated. The time values in this figure are taken from the table by Nieuwkoop and Faber (41).

Faber (41). In our experiments there was variation in the speed of development from batch to batch, but there was a rough agreement with their table.

Development of ACh Sensitivity in Cultured Cells

158 myotome cells developing in culture between corresponding stages 19–46 were impaled with microelectrodes and tested for the presence of ACh sensitivity. Cells that responded to iontophoretic application of ACh at one surface point always gave further responses at other positions on the surface. Some cells did not respond with an obvious depolarization (>1 mV) to ACh application regardless of the position of the pipette or the current intensity used. We judged these cells nonsensitive. In Fig. 3 the frequency of occurrence of sensitive cells (without regard to the degree of sensitivity) was plotted against the corresponding stage of cultured cells. The ACh sensitivity first emerged at corresponding stage 20; at stages 27 and thereafter almost all muscle cells showed sensitivity.

In 51 myotome cells, the degree of ACh sensitivity was measured quantitatively. When the iontophoretic electrode was placed so that it was barely touching the cell surface, the application of ACh caused a quickly rising depolarization (ACh potential) (Fig. 4*A*). Examples of the relation between the electrical charge (Q) through the pipette and the peak depolarization are shown in Fig. 4*B*. The maximum slope of these curves are defined as the ACh sensitivity (in millivotts

and averaged. The average variation for different positions on per nanocoulomb) (30). For each cell the sensitivity was measured at one to seven (average two and one-half) positions

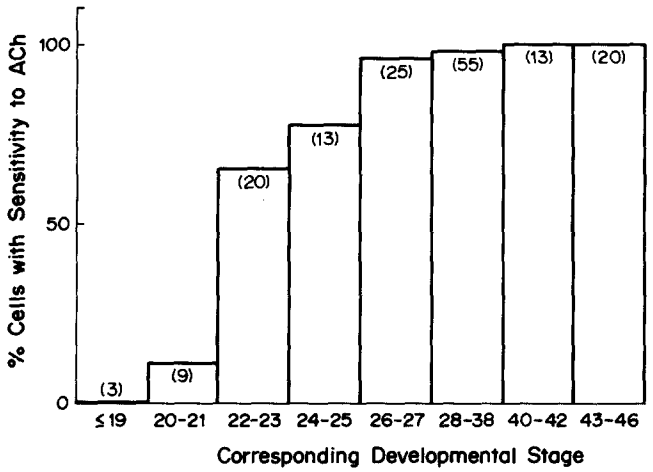

FIGURE 3 The relation between corresponding developmental stage and the percentage occurrence of acetylcholine-sensitive cells in cultured *Xenopus* embryonic muscle. Cells were judged nonsensitive if they did not respond to iontophoretic application of ACh with more than 1 mV depolarization (tested on at least two different positions). The number of cells tested is indicated in the parenthesis.

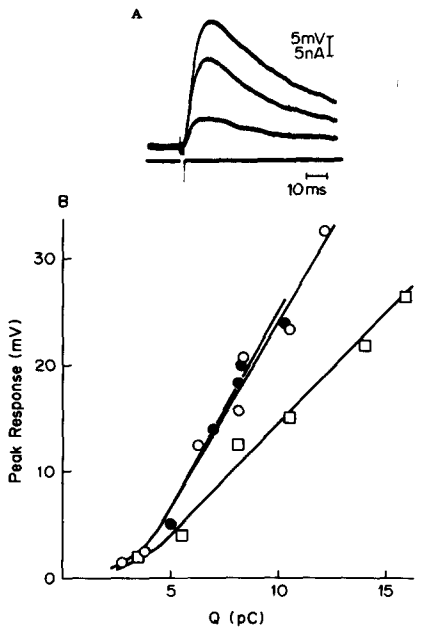

FIGURE 4 Quantitative measurement of acetylcholine sensitivity using the slope method. (*A*) A sample recording from the single point on a cell, in which three different sized current pulses (the second and third are obscured by the potential trace) were applied through the acetylcholine chloride iontophoretic pipette. The upper traces show membrane potential changes (acetylcholine potentials) and the lower traces represent currents through the pipette. Three separate records were superimposed photographically. Resting potential was −80 mV. Stage was 42. (*B*) Sample dose-response curves from a different cell. Abscissa is the electrophoretic quantity (in picocoulombs) and the ordinate is the amplitude of the acetylcholine potentials. Three different points on this cell were tested. The maximum slope of the curve is the quantity used to express the sensitivity in millivotts/nanocoulomb. In many cells, as in this example, the relationship was linear up to 30 mV depolarization despite the expected nonlinear relation. The resting potential was −80 mV. Stage 32/33.

a single cell was ± 21%. Cells at early developmental stages tended to have lower resting potentials than cells at later stages (~ −30 mV at stage 20, and −80 mV at stages 42 and thereafter). We are not sure whether this difference is real; some of the difference could be due to the higher input resistance in younger cells. The cells with low resting potentials were hyperpolarized to ~ −60 mV by injecting current into the cell using the bridge circuit before starting the measurement of the sensitivity. Because the membrane potential and input resistance affect the magnitude of ACh induced depolarization, the sensitivity of each cell was normalized to a standard cell which has input resistance of 165 MΩ (average input resistance of the sample) and membrane potential of −80 mV, assuming that the reversal potential was 0 mV. Thus, the normalized sensitivity is $S_n = S(V_s/V)(R_s/R)$, in which V_s is the standard membrane potential, V is the measured resting potential, R_s is the standard input resistance; R is the measured resistance, and S is the measured sensitivity (29). The normalized value thus obtained would reflect the ACh sensitivity of the cell per unit surface area.

The normalized ACh sensitivities at various developmental stages are shown in Fig. 5 *A*. In this figure we did not include the data of nonsensitive cells. Thus, the figure indicates that

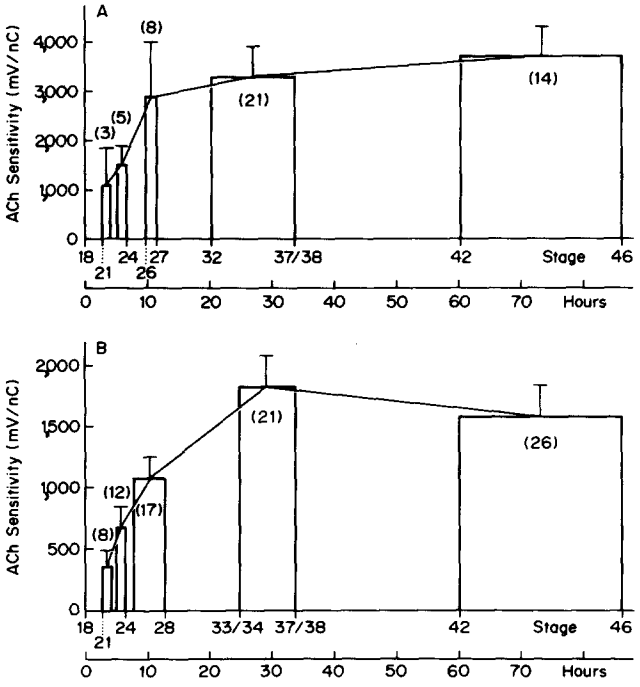

FIGURE 5 Change in the acetylcholine sensitivity of cultured muscle cells with development. The sensitivity for each developmental period was obtained as follows. The mean acetylcholine sensitivity for each cell was calculated by averaging the sensitivities measured at different test points (see Fig. 4). A mean acetylcholine sensitivity for each developmental period was obtained by averaging the mean sensitivities for the individual cells. The developmental stage for each cell was determined as explained in the text (except for eight cells, in which we estimated the stages from the standard table; 41). The linear time scale of abscissa was drawn from the Nieuwkoop and Faber table. The number of cells tested is shown in parenthesis. Cells without acetylcholine sensitivity were not included. Bars represent SEM. (*A*) Data from the 1980 experiments; the same cells were used for freeze-fracture. (*B*) Data from the 1982–1983 experiments; only electrophysiological experiments were done.

the degree of ACh sensitivity (as well as the proportion of the cells with sensitivity) increases as development proceeds.

Further Experiments on ACh Sensitivity in Cultured Cells

The data of Fig. 5*A* were obtained from January to April 1980. In these experiments after the determination of ACh sensitivity, the same muscle cells were used for morphological investigation (see below). The experiments were difficult, the resulting number of data is not large (particularly at early stages), and there was uncertainty in estimating the input resistance in some cells (see Materials and Methods). Thus, from March 1982 to January 1983, we accumulated more data on ACh sensitivity (physiology experiments only).

We did experiments on seven batches of embryos. We did not include the data of one batch, because in this batch the sensitivity in one cell was absent even at stage 33/34, indicating an unhealthy development. In the remaining six batches, all the cells tested after stage 21 had ACh sensitivity. The sensitivities were again normalized to the condition of −80 mV resting potential and 165 MΩ input resistance, and the data are shown in Fig. 5*B*.

Comparison of Fig. 5*A* with *B* shows that the ACh sensitivity in both sets of experiments developed with similar time courses (except that the overall sensitivities in *B* are lower than those in *A*). Thus, from the results of Fig. 5*A* and *B*, together with those in Fig. 3, we can conclude that the ACh sensitivity appears for the first time at stage 20, in agreement with Blackshaw and Warner (4), and thereafter it increases over the next 20 h up to about stage 32. We are unable to explain why the overall values of sensitivity were lower in the 1982–1983 experiments than those in the 1980 experiments. The differences in experimental conditions (such as the size of *Xenopus* and the different batches of the drug ACh used) failed to explain the discrepancy. One possibility is that in the 1982–1983 experiments, the technique of isolating myotome cells at early stages (14–16) became so good that it produced purer muscle cell cultures with less fibroblast contamination: the contamination with fibroblast elements could influence the development of ACh sensitivity.

Dispersed and Aggregated Particles on Cultured Cells

The presence of aggregates of large intramembraneous particles has been described in cultured *Xenopus* myotome cells (43, 44). These aggregates of large particles, also found in cultured chick myotubes, have been shown to represent dense conglomerations of ACh receptors (hot spots) (12, 53). In our cultures these aggregates occurred only in cultured cells at advanced stages. Cells younger than corresponding stage 31 did not have these particle aggregates. The membrane of isolated cells during these initial stages contained only diffusely distributed particles (Fig. 6*A* and *B*). At the corresponding stages 32–34, however, small scattered aggregates of large particles began to appear, and at corresponding stages 36–46, ~60–75% of the cells contained distinct clusters of particle aggregates (Fig. 6 *C* and *D*). However, even at stage 46, the membrane area occupied by the aggregates remained fairly small, and was only 1–2% of the total cell surface.

The primary purpose of the present experiments was to compare the ACh sensitivity with the density of dispersed particles. In the electrophysiological experiments described above, it is likely that almost all the records were obtained from the diffusely sensitive regions, in that the area occupied by hot spots is very small (1–2% in our cells of stages 36–46, and 1.7% in Moody-Corbett and Cohen's sample [39]). Rarely we encountered a very high sensitivity of more than 10,000 mV/nC (normalized value), which may have been recorded from hot spots. Eliminating these records, however, produces only small differences in the data of Fig. 5*A*.

Dispersed Particles at Various Stages in Culture

11 cells from corresponding stages 19–24, in which physiological tests had established that they were nonsensitive to ACh, were successfully fractured and identified in replicas. Fig. 7 shows an example, in which the light microscopic picture, taken immediately after the sensitivity test, can be seen to correspond with the freeze-fracture view. High magnification of the fractured surface of the membrane (Fig. 6*A*) shows solitary particles scattered over the surface. The size distributions of dispersed particles from these cells are shown in solid circles of Fig. 8*A*. Particle diameters ranged from 4 to 18 nm with a peak at 8 nm. The average total particle density was 712 ± 66/μm^2 (mean ± SEM).

We succeeded in obtaining freeze-fracture replicas of 26 cells (stages 22–46), which were sensitive to ACh. For each cell, the ACh sensitivity was measured quantitatively. An example of the fractured surface is displayed in Fig. 6*B*, and the average size distribution of the dispersed particles for this sample is plotted by the open circles (○) of Fig. 8*A*. Particle diameter ranged from 4 to 20 nm with the peak at 9 nm. The average total particle density was 1,086 ± 49/μm^2 (mean ± SEM).

Comparison of the two curves in Fig. 8*A* indicates that there is essentially no difference in the density of small sized particles (8 nm and below). But there is a definite increase in the population of large particles as the cell acquires ACh sensitivity, and the population of the particles of >12 nm increased roughly two times (also compare the replicas in Fig. 6*A* and *B*). In Fig. 8*B*, we plotted the differences between the two curves of Fig. 8*A*. We will refer to this population of particles, which constitute the difference between the particles of sensitive cells and those of the nonsensitive cells, as difference particles. The sizes of difference particles are between 8 and 20 nm with a peak at 11 nm. The total density of the difference particles in this sample was 353/μm^2, which is 33% of the total particle density.

Difference Particles at Various Stages in Culture

In Fig. 9, the difference particles were plotted for various corresponding culture stages. This sample includes only those cells that had ACh sensitivity, and is the same sample as that indicated by the open circles (○) in Fig. 8*A* (i.e., a subset of the sample in Fig. 5*A*, in which freeze-fracture was successful). It is seen that the density of the difference particles increases as development proceeds. At culture stages 22–24, the particle density was 100/μm^2, whereas at culture stages 33–46, it attained the value of ~500/μm^2.

Correlation Between ACh Sensitivity and the Density of Difference Particles

The ACh sensitivity increased as development proceeds (Fig. 5). The density of difference particle also increased with

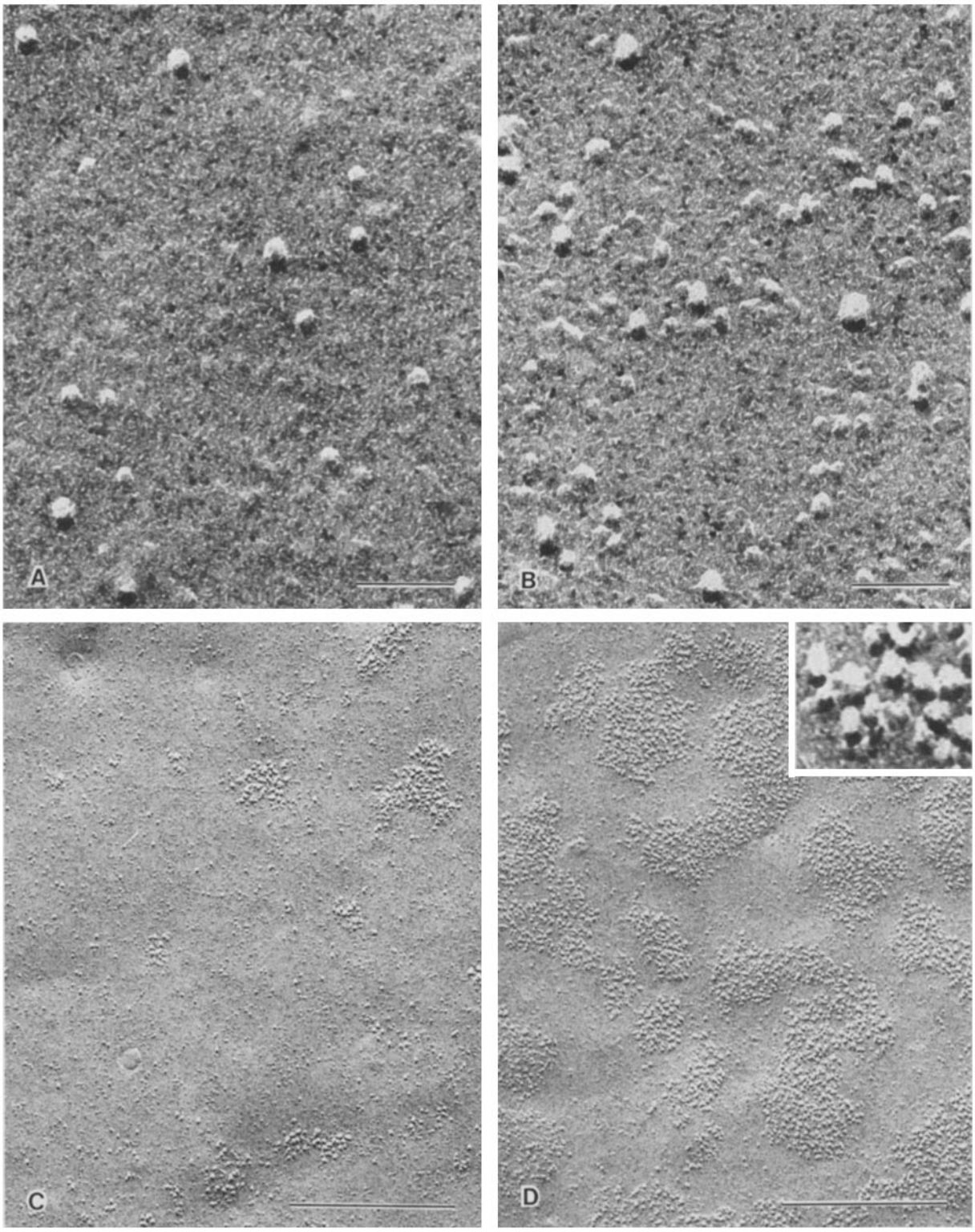

FIGURE 6 Freeze-fracture electron microscopy. *A* and *B* are high-magnification views of dispersed P-face particles. (*A*) Stage 22 cell without sensitivity to acetylcholine; (*B*) stage 32 cell with an average ACh sensitivity of 1,000 mV/nC. *C* and *D* show ACh receptor P-face particle aggregates during cluster formation. (*C*) Stage 32 cell. Small aggregates are loosely distributed over a wide area of the cell surface. (*D*) A more mature cell (stage 36). Aggregates are now tightly clustered together in a relatively small area or plaque on the cell surface. Inset shows a high magnification of the aggregated particles. Bars, 0.05 μm (*A*, *B*, and *D*[*inset*]); 0.5 μm (*C* and *D*). × 319,000 (*A* and *B*); × 54,000 (*C* and *D*); × 319,000 (*inset*).

development (Fig. 9). Thus, it is natural to expect that there would be a positive correlation between the ACh sensitivity and the density of difference particles (regardless of the stage). Table II, which was taken from the cell sample of Fig. 9, shows that this is indeed the case.

Dispersed Particles on the Top and the Bottom Surfaces of Cultured Cells

In the double-replica method of freeze fracture used in this study, most of fractures occurred through the membrane

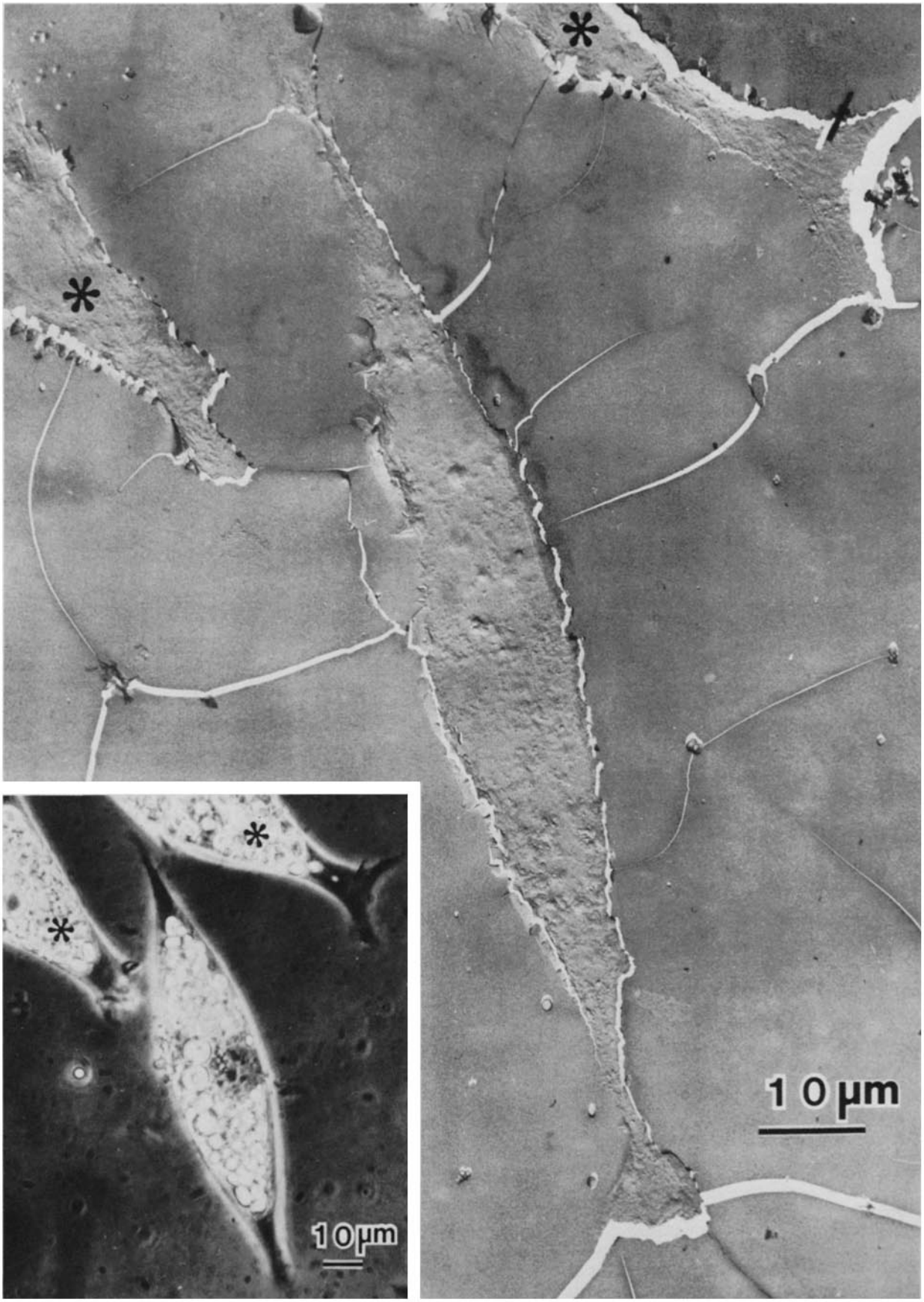

FIGURE 7 Identification of cells in freeze-fracture replicas. A cell at stage 21, which did not have acetylcholine sensitivity, is shown in both a freeze-fracture replica and a phase contrast micrograph (*inset*). The asterisk indicates two adjacent cells used for orientation. Cells were photographed immediately after physiological recording, fixed, and processed for freeze-fracture. Identification in replicas was facilitated by using EM grids with large open areas (Ted Pella, Inc., Tustin, CA). × 1,900. × 700 (*inset*).

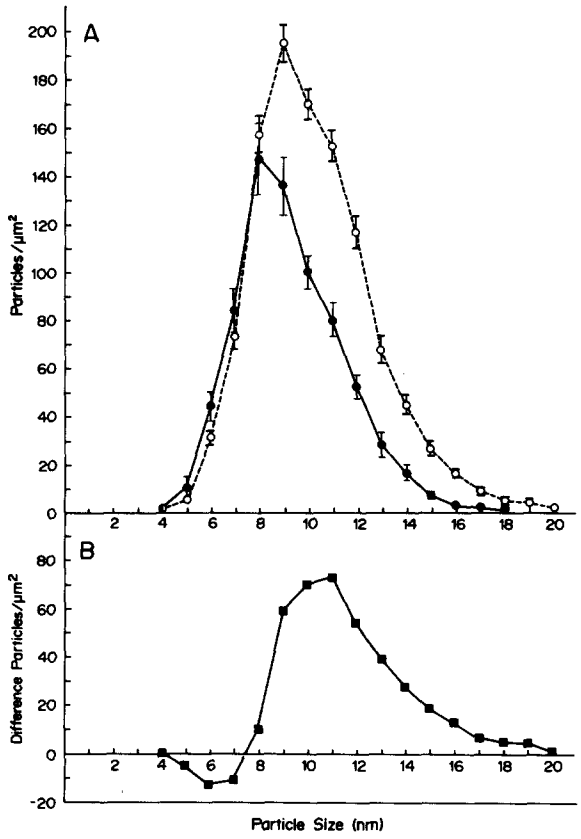

FIGURE 8 Size distribution histogram of P-face dispersed particles in cultured muscle cells. (A) ●, histogram for nonsensitive cells between stages 20–24. 11 cells were analyzed. Total number of particles measured is 6,189. Average total particle density was 712 ± 66 particles/μm^2 (mean ± SEM). The average particle size was 9.4 ± 0.3 nm. (A) O, histogram from sensitive cells. 26 cells between stages 21 and 46 were analyzed. Total number of particles measured was 22,648. The average particle size was 10.4 ± 0.3 nm, and the average particle density was 1,086 ± 49 particles/μm^2. (*B*) Difference between the two distributions shown in *A*. We call this group difference particles.

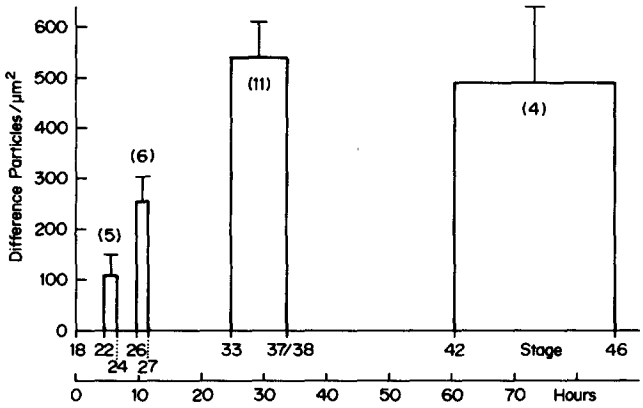

FIGURE 9 Change in the density of difference particles with development. The average particle distribution of nonsensitive cells (● in Fig. 8*A*) was subtracted from the distribution found on each cell with sensitivity. The density of difference particles of each cell was then used to calculate the average density for each developmental period. The vertical bars represent the SEM. The number in parenthesis indicate the number of cells.

facing the bottom of the culture dish. In contrast, the ACh sensitivity was measured on the top side of the cell membrane. This is a limitation of the present study. However, in one cell

TABLE II

ACh Sensitivity vs. Difference Particles

Difference particles/μm^2	ACh sensitivity		*n*
	mV/nC	*SEM*	
0–200	1,270	±450	8
300–800	3,690	±670	18

Relation between acetylcholine sensitivity and the density of difference particles (regardless of stage). The data in this table were taken from the cell sample shown in Fig. 9. Cells with a higher density of difference particles have a significantly ($P < 0.05$) greater sensitivity.

(stage 36), in which the ACh sensitivity was quantitatively tested, a cross-fracture occurred, revealing portions of the top and bottom membrane P faces. The densities and the distribution of the diffusely distributed particle size were almost the same on both membranes of the cell. This result suggests that there would not be a marked difference in the dispersed particles between the two sides, although it has been reported that there are differences in the way hot spots distribute (6, 38).

Size Distribution of Various Particles

In Fig. 10, we summarize the size distribution of various particles seen in cultured *Xenopus* muscle cells. The particle size in a freeze-fracture replica does not, of course, represent the real size of the protein molecule. Nevertheless, the comparison of particle sizes in replicas produced under the same conditions should give a semiquantitative evaluation of the relative size of various groups of membrane proteins.

The open squares (□) of Fig. 10 represent nonspecific dispersed particles, which were taken from the ACh nonsensitive cells (as were the filled circles (●) of Fig. 8*A*). They are a group of particles with the smallest sizes, having a peak of 8 nm. The filled triangles (▲) are particles from gap junctions between two myotome cells, which were present in the replica of muscle cells in contact with each other. These particles exist in very dense aggregates (5,670/μm^2), and show a sharp peak at 9 nm, indicating that the size of each particle is relatively uniform. The filled circles (●) are from the clusters of particle aggregates, which most probably represent the aggregates of ACh receptors (hot spots) (12, 43, 53). The size of the particles in this group is the largest seen on the fractured membrane P face. Their size distribution extends rather broadly, and the density is quite high (2,300/μm^2). The particle aggregates of putative ACh receptors seen in the subsynaptic membranes (either embryonic or adult *Xenopus* muscle) show almost the same size distribution (44; Bridgman, unpublished results). The open circles (○) represent the difference particles (the difference between ACh sensitive and nonsensitive cells). These particles are large, with a peak at 11 nm but they are not quite as large as those of the hot-spot particles.

Development of ACh Sensitivity in Embryonic Muscle In Situ

It could be argued that the results on cultured materials might not be readily applicable to naturally developing embryonic cells. We, thus, performed the same sort of experiments using myotome cells in situ, despite the difficulty in interpreting the results in quantitative terms. The difficulty arises from a poor visibility of the individual myotome cells and an extensive electrical coupling (5).

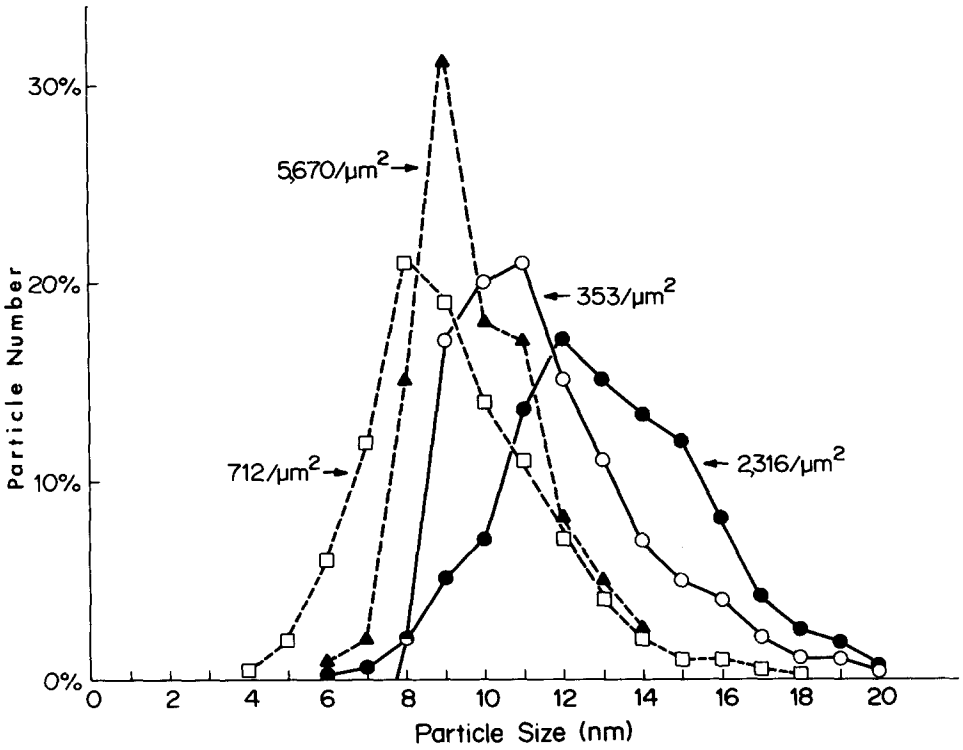

FIGURE 10 A summary of the size distributions of various particle populations found on cultured *Xenopus* muscle cells. ●, the distribution in receptor aggregates (average distribution from six different aggregates; total number of particles measured: 703). ○, difference particles (same as the distribution in Fig. 8*B*). ▲, gap-junction particle aggregates found between two muscle cells (from a single aggregate; total number of particles meaasured: 151). □, nonspecific particles found on cells without acetylcholine sensitivity (same as ● in Fig. 8*A*). The ordinate is the number of particles in percent of the total counted for each group. The number for each curve indicates the total density of particles. ●, AChR aggregates; ○, AChR dispersed + ?; ▲, gap junction aggregates; □, no ACh sensitivity.

The myotomes of *Xenopus* embryos are arranged in a series of short segments containing parallel rows of muscle cells (see Fig. 14*A*). These cells receive innervation at both ends (35). Development of the segments starts at the head and proceeds caudally (4, 20, 41). For these reasons, electrophysiological experiments were done on myotomes located at the first to the fourth rostral segments, and similarly the freeze-fracture survey on dispersed particles was made on material taken at the ends of the cells located in rostral segments.

Myotome cells from 33 embryos at relatively early stages (between stages 19 and 25) were impaled with microelectrodes and tested for ACh sensitivity. Fig. 11 *B* shows a cell in which a drop of ACh into the superfusion system caused a transient depolarization (ACh-potential). In the example shown in Fig. 11*C*, the ACh potential was elicited in a cell that had spontaneous endplate potentials. Some cells did not respond to ACh (Fig. 11*A*) even with a dose of four drops. In Fig. 12 the percentages of embryos that responded to ACh are plotted against developmental stages. The hatched area of each column indicates the percentage of cells that had spontaneous endplate potentials and had ACh sensitivity, whereas the open area indicates the cells that had ACh sensitivity without the spontaneous endplate potentials. ACh sensitivity started to appear at stage 20. This result is essentially in agreement with that obtained from cultured cells (Fig. 3), and is in keeping with the data reported for *Xenopus* embryonic muscle cells by Blackshaw and Warner (4) and Kullberg et al. (31).

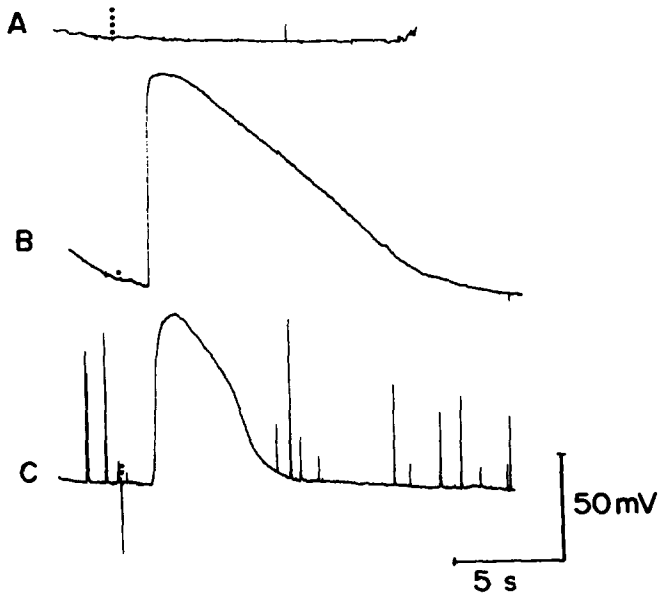

FIGURE 11 Tests for acetylcholine sensitivity in *Xenopus* embryo muscles in situ. (*A*) A recording from an embryo (stage 21) that showed no response to acetylcholine. (*B*) A recording showing a large depolarization indicating sensitivity to acetylcholine (stages 20–21 embryo). (C) A recording from an embryo (stage 23) that responded with a large depolarization and also showed spontaneous endplate activity. Dots indicate the number of drops of 10^{-4} g/ml acetylcholine, which were introduced into the superfusion system. Resting potentials in *A* was −80 mV, in *B* was −115 mV, and in C was −99 mV.

Particle Size Distribution in Embryonic Muscles In Situ

The filled circles (●) in Fig. 13*A* show the size distribution of dispersed particles on myotome cell membrane from nine embryos (stages 19–23) that were nonsensitive to ACh (sample picture is in Fig. 14*B*). The particle size ranges from 5 to 16 nm, and the peak was located at 9 nm. The open circles (○) of Fig. 13*A* are the particle size distribution taken from 12 embryos (stages 20–24) that had ACh sensitivity (sample picture in Fig. 14*C*). In Fig. 13*B*, we plotted the differences between the two curves in Fig. 13*A*. It is seen that the difference distribution ranges from 9 to 18 nm with a peak at 12 nm. These results are similar to that obtained for the cultured cells. The less obvious difference between the two curves in Fig. 13*A* compared with those in Fig. 8*A* may result from the greater ambiguity associated with correlating ACh

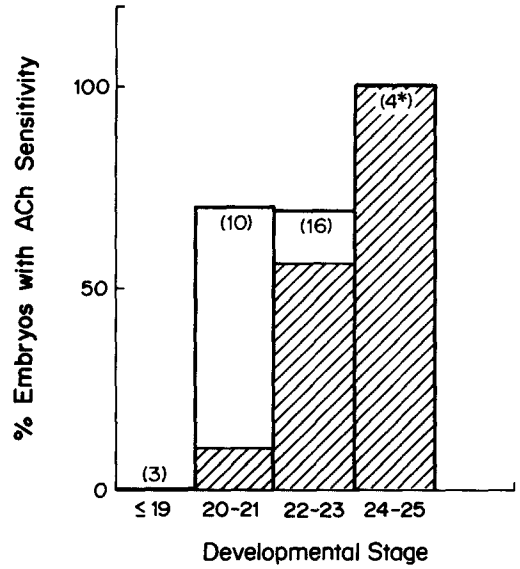

FIGURE 12 Development of acetylcholine sensitivity in *Xenopus*. Open areas indicate the percentage of embryos that had cells with ACh sensitivity but no spontaneous endplate potentials. Hatch marks indicate the percentage of embryos that also showed spontaneous endplate activity. The number of embryos tested at each developmental period is indicated in parentheses. (*4**) At stages 24–25, most embryos already showed movement indicating functional innervation; therefore, only embryos that did not show movement at these stages were tested.

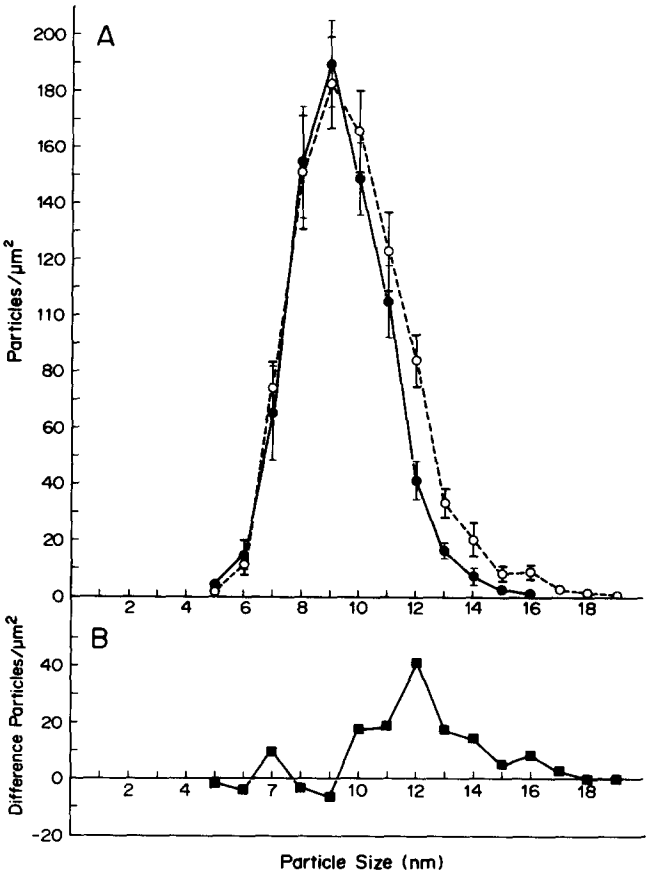

FIGURE 13 Size distribution histogram of P-face dispersed particles in myotome cells of embryos in situ. (*A*) ●, histogram from nonsensitive cells. Data from seven embryos between stages 19–23. Total number of particles measured was 1,322. The average particle size was 9.0 ± 0.2 nm (mean ± SEM), and the average total particle density was 746 ± 57 particles/μm^2. (*A*) ○, histogram from sensitive cells. Data from 12 embryos between stages 20 and 24. Total number of particles measured was 2,915. The average particle size was 9.5 ± 0.2 nm. The average total particle density was 810 ± 70 particles/μm^2. (*B*) The difference between the two distributions shown in *A*.

sensitivity and particle density in embryos. We could not measure particle diameters in the same cell that we tested electrophysiologically. It is therefore possible that in some cases we measured particle diameters from cells that had gained functional ACh receptors even though our electrophysiological assay for the embryo gave negative results. This would cause contamination of the particle density distribution of nonsensitive cells causing a shift in the distribution to the right. Particle aggregates resembling the putative ACh receptor aggregates were also seen on myotome cells from embryos at these early stages (Fig. 14 *D*). These aggregates, however, were found only in embryos from which spontaneous endplate potentials were recorded, suggesting a postsynaptic origin. In summary, although the in situ experiments on myotome cells are not as quantitative as those on cultured cells, the data on particle size are in essential agreement with those from cultured cells.

DISCUSSION

Interpretation of Freeze-Fracture Particles

Freeze-etch data have established that ACh receptors of *Torpedo* electroplaques and muscles are represented by 8.5-nm surface projections with a density of ~10,000/μm^2 (23, 24). By comparison, the density of α-bungarotoxin binding sites in muscle subsynaptic membrane is about 18,000/μm^2 (33, 37). Because two α-bungarotoxin molecules bind to one ACh receptor molecule, ACh receptor density would be ~10,000/μm^2. Thus, each surface projection seen in freeze-etching would correspond to one ACh receptor molecule. Freeze-fracture of subsynaptic membranes, on the other hand, reveals large intramembrane particles (mostly on the P face, only a few on the E face) with a total density of only about 5,000/μm^2 (23). Heuser and Salpeter's (23) interpretation of this discrepancy is that some of the ACh receptors are not detected after fracture because the fracture plane goes through the middle of the receptor molecules and the resulting particle is too short to see against the background plane. This interpretation indicates that each of the large particles in the fractured subsynaptic membrane can still be regarded as representing one ACh receptor molecule, but that the real receptor density would be roughly twice as high as the intramembrane particle density. We assume that the same situation would obtain in the diffusely distributed ACh receptors.

ACh Receptors and Difference Particles

We have observed that in *Xenopus* muscle the critical developmental time for ACh receptors to become detectable by the physiological technique is stage 20. This was independent of whether the cells were tested in situ or after culturing. After this initial appearance of ACh sensitivity, the sensitivity in culture gradually increased over the next 20 h. Observation of membrane ultrastructure revealed that young cells that were nonsensitive to ACh had intramembraneous particles of relatively small size scattered over the membrane. As the cells developed and acquired ACh sensitivity, a different group of particles, which were larger in size, began to appear. We designated these particles difference particles. The density of

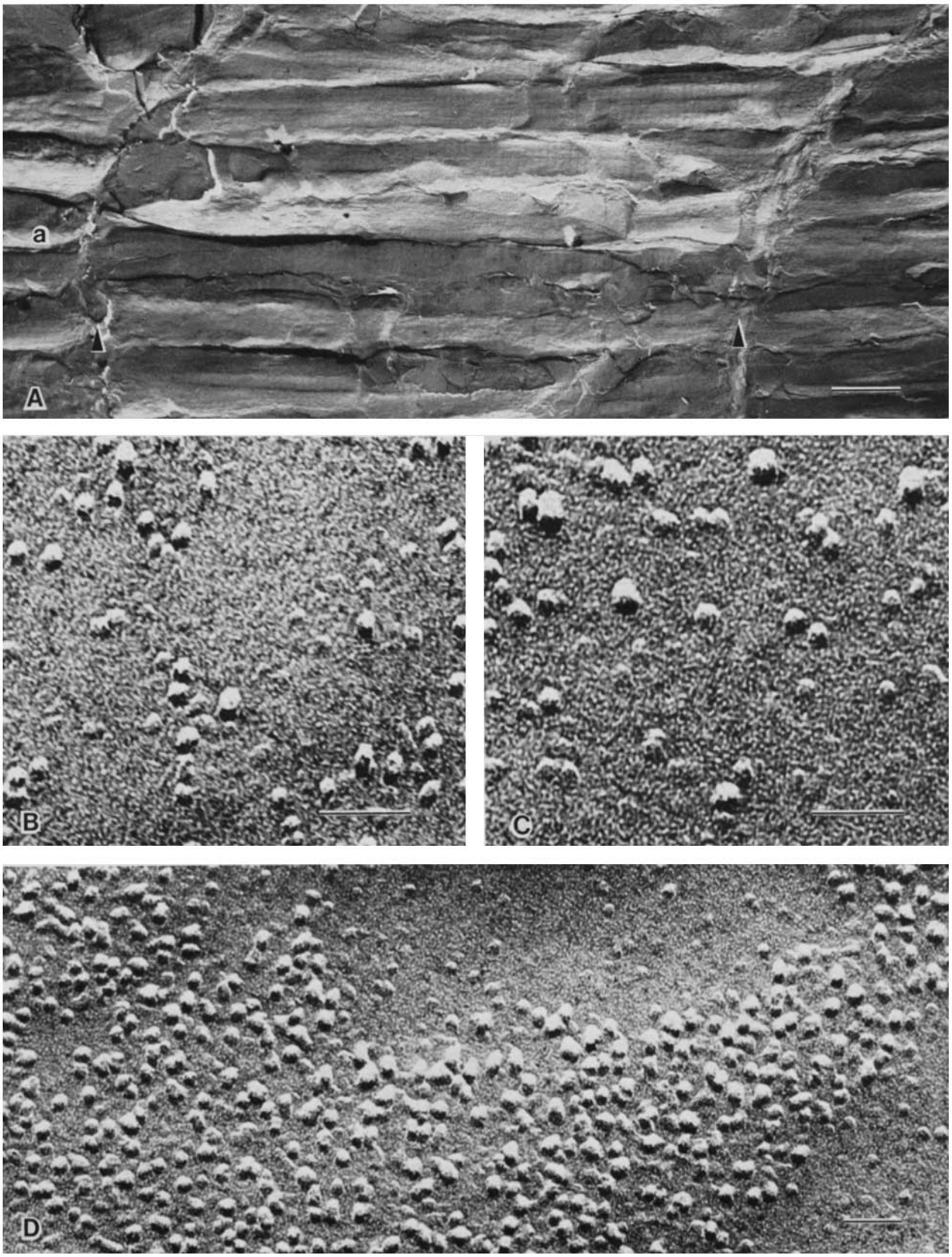

FIGURE 14 Freeze-fracture electron microscopy of myotome muscle in situ. *A* is a low magnification view of the *Xenopus* myotome muscle. The short mononucleated cells are arranged in segments. The boundaries of the segments are indicated by arrowheads. Rostal side of the body is indicated by *a*. (*B*) High-magnification view of the P face of a myotome cell from stage 22 embryo without sensitivity to ACh. (C) A high-magnification view of the P face of a myotome cell from a stage 22 embryo with sensitivity to ACh. (D) A putative acetylcholine receptor particle aggregate on a *Xenopus* myotome muscle cell. From a stage 21 embryo that had both ACh sensitivity and spontaneous endplate potentials. Aggregates were found at the ends of several cells in an anterior segment. Bars, 10 μm (*A*); 0.05 μm (*B–D*). × 1,200 (*A*); × 319,000 (*B* and C); × 193,000 (*D*).

the difference particles gradually increased with development, from 100/μm^2 at stages 22–24, reaching 500/μm^2 at stages 33–46. (These values of the density are on the same order of magnitude as the densities of α-bungarotoxin binding sites in non-hot spot areas of L-6 myotubes [5–400 sites/μm^2] or of primary rat myotubes [54–900 sites/μm^2] obtained by Land et al. [32].) Because the timing of the initial increase and subsequent plateau in both the ACh sensitivity and the density of difference particles was very close, we suggest the possibility that these two processes are linked. The simplest explanation for our results is that functional ACh receptors have been inserted into the membrane as development proceeds and are represented in freeze-fracture replicas as particles that contribute to the population of difference particles. This explanation is only plausible, however, if it is assumed that ACh receptor particles contribute to the population of difference particles (more about this point later) and the preexisting particles that were present in nonsensitive cells do not undergo a continuous size change with development.

It is known that the dense assembly of ACh receptors located at neuromuscular junctions or in hot spots are seen, in freeze-fracture replicas, as clustered aggregates of large particles (12, 22, 43, 45, 53). In our study such aggregates contained particles that constituted the largest sizes seen on the muscle cell surface (Fig. 10, ●). This size distribution did not exactly coincide with that of the difference particles (Fig. 10, ○). One way to interpret this discrepancy is to suppose that each ACh receptor becomes slightly larger as it matures and starts forming an aggregate. Another possibility is that our difference particles consist of ACh receptors and other integral membrane proteins. It is quite possible that as the cells develop, the densities of other integral proteins, such as sodium or potassium channels, increase. Interestingly, the intramembraneous particles at the node of Ranvier, which could contain the Na channels and K channels, are quite large in size (9–11 nm), but slightly smaller than the putative ACh receptors in aggregates (51), although it is not justified to emphasize small differences in freeze-fracture pictures from different laboratories. We do not know which of the alternatives is correct. At present we prefer the second one because it involves less unproven assumptions.

One question to be considered is what proportion ACh receptor particles would occupy among the total population of difference particles. Our data show that the density of difference particles reaches 500/μm^2 at stages 33–46 (Fig. 9). The density of particles of clusters of aggregates (hot spots) was 1,700/μm^2. Thus, the ratio of the densities is roughly 1:3. Kidokoro and Gruener (28) studied the α-bungarotoxin binding sites of embryonic *Xenopus* muscle cultures (somewhat older stages than ours) by means of autoradiography. They showed that the density of the binding sites at diffuse areas was ~100/μm^2, whereas that at hot spots was ~900/μm^2, the ratio being 1:9 (in disagreement with Anderson et al. (2), who reported that the density of the binding sites at diffuse areas are only 4% of that at hot spots). Although the calibration of the absolute densities of the binding sites was not done in the Kidokoro and Gruener (28) study, the ratio of the densities would be reliable. Thus, if all the particles in hot spots are assumed to represent ACh receptors, about one-third of the difference particles could be the ACh receptors.

Another way of estimation is to correlate electrophysiological data (ACh sensitivity) with our particle data. According to Gruener and Kidokoro (19), the ACh sensitivity of the background region was 1.7 mV/pC and that of hot spots was 5.0 mV/pC in the cultured *Xenopus* embryonic muscle cells: hence, the ratio of the sensitivities is 1:3. Inasmuch as the ratio of the particle densities is also 1:3 (present data), the results suggest that almost all the difference particles could consist of ACh receptors. The same conclusion is obtained by comparing the sensitivity data and particle density data in junctional and nonjunctional regions; the data are in Gruener and Kidokoro (19), Peng & Nakajima (43), and the present experiments.

In sum, the above estimate indicates a possibility that a substantial proportion (⅓ to 1) of the difference parrticles represents the diffusely scattered ACh receptors. However, we are not sure how reliable these estimates are because they are dependent on an assumption that all particles in *Xenopus* hot spots consist of ACh receptors. If only one-half of the particles in the hot spot represented ACh receptors, the estimate of the proportion would become only ⅙ to ½. In *rat* myotubes, however, Pumplin and Drachman (46) reported that the particle density within the hot spot was 750–1,000/μm^2; this value pertains to the total area of the hot spot, not to each region of an aggregate. In that freeze-fracture particles may represent about one-half of the real receptor density (23) the receptor density may be 1,500–2,000/μm^2. Land et al. (32) reported that α-bungarotoxin binding sites in hot spots in *rat* myotubes was 3,000–4,000 sites/μm^2 (they calibrated the absolute value carefully). Because two α-bungarotoxin molecules bind to one ACh receptor, this indicates the density of 1,500–2,000 receptors/μm^2. This exact coincidence of the two sets of data could be fortuitous; nevertheless, it indicates that at least in rat myotubes, most of the hot spot particles could represent ACh receptors. Similar data are not available in *Xenopus* cultures.

Function of Solitary ACh Receptors

In spite of the uncertainty about the conclusion of the previous section, the following statement is likely true; namely, functional ACh receptors at initial stages are contained in the difference particles. The difference particles existed almost always in solitary form (some in double). We did not observe microaggregates (consisting of several particles) scattered throughout the surface membrane. Thus, an ACh receptor probably can function in unitary (or dimeric) form without cooperative actions from several other ACh receptors. Although previously silver grains from ^{125}I-α-bungarotoxin autoradiography were known to exist in scattered form, the autoradiographic data cannot be taken as indicating the existence of solitary binding sites. Although biochemical work indicates that ACh receptor molecules from *Torpedo* electroplaques exist in a dimeric form, recent evidence suggests that ACh receptors from muscles exist mostly in monomeric form (36).

Gradual Development of ACh Sensitivity

Blackshaw and Warner (4) reported that in *Xenopus* embryo muscles "ACh receptors become functional relatively quickly" (at stages 21–22) and observed that "the response is immediately established at the maximum level." They called this process ACh receptor activation. (See Ohmori and Sasaki [42] for another example of rapid development of ACh sensitivity.) Blackshaw's and Warner's result could be explained by hypothesizing the existence of an inactive form of ACh receptors. Many ACh receptors would be inserted into the membrane in inactive form before stage 20, and at stage 20

all of them would be suddenly "activated." Our present results on cultured cells show that indeed the first emergence of functional ACh receptors occurs at stage 20, but that the sensitivity gradually increases over the next 20 h (up to about stage 32). Together with the increase of sensitivity, the density of difference particles also increases. Our results can be explained by the following alternative schemes: (*a*) The first insertion of ACh receptors takes place near stage 20. Each ACh receptor becomes functional soon after the insertion, the insertion of receptors continues, and a maximum density is attained at stage 32. (*b*) The first insertion of ACh receptors takes place before stage 20, but they are still in inactive form. At stage 20, they are activated; thereafter, the gradual insertion and the activation continue.

It would be unwise to speculate further. The macroscopic sensitivity is a complicated quantity, which depends not only on the density of the receptors on the surface, but also on the kinetic properties of the gating and the single-channel conductance. Now that we have described the functional and structural developmental sequences of this culture system in detail, it offers excellent material to investigate changes of functional characteristics of each ACh receptor after its insertion into the cell membrane.

We thank Dr. H. B. Peng for his help in constructing the bridge circuit used in our experiments.

This research was supported by Grants NS-10457 and NS-08601, and Training Grant T32-GM-07211 from the National Institutes of Health, and a grant from the Muscular Dystrophy Association.

Received for publication 11 July 1983, and in revised form 9 February 1984.

REFERENCES

1. Anderson, M. J., and M. W. Cohen. 1977. Nerve-induced and spontaneous redistribution of acetylcholine receptors on cultured muscle cells. *J. Physiol. (Lond.).* 268:757–773.
2. Anderson, M. J., M. W. Cohen, and E. Zorychata. 1977. Effects of innervation on the distribution of acetylcholine receptors on cultured muscle cells. *J. Physiol. (Lond.).* 268:731–756.
3. Bevan, S., and J. H. Steinbach. 1977. The distribution of α-bungarotoxin binding sites on mammalian skeletal muscle developing *in vivo*. *J. Physiol. (Lond.).* 267:295–213.
4. Blackshaw, S. E., and A. E. Warner. 1976a. Onset of acetylcholine sensitivity and endplate activity in developing myotome muscles of *Xenopus*. *Nature. (Lond.).* 262:217–218.
5. Blackshaw, S. E., and A. E. Warner. 1976b. Low resistance junctions between mesoderm cells during development of trunk muscles. *J. Physiol. (Lond.).* 255:209–230.
6. Bloch, R. J., and B. Geiger. 1980. The localization of acetylcholine receptor clusters in areas of cell-substrate contact in cultures of rat myotubes. *Cell.* 21:25–35.
7. Bridgman, P. C., and A. Greenberg. 1979. A correlation between the appearance of 11–19 nm intramembrane particles and acetylcholine sensitivity in *Xenopus* embryonic muscle. *Soc. Neurosci. Abstr.* 5:476.
8. Bridgman, P. C., S. Nakajima, A. Greenberg, and Y. Nakajima. 1981. Intramembrane particles of cultured embryonic muscle and their relationship to acetylcholine sensitivity. *Soc. Neurosci. Abstr.* 7:702.
9. Bridgman, P. C., S. Nakajima, A. S. Greenberg, and Y. Nakajima. 1982. Structure and function of embryonic acetylcholine receptors in dispersed form in *Xenopus* muscle. *Biophys. J.* 37:17a. (Abstr.)
10. Burden, S. 1977. Development of the neuromuscular junction in the chick embryo: the number, distribution, and stability of acetylcholine receptors. *Dev. Biol.* 57:317–329.
11. Cartaud, E., L. Bendetti, J. B. Cohen, J. C. Meunier, and J. P. Changeux. 1973. Presence of a lattice structure in membrane fragments rich in nicotinic receptor protein from the electric organ of *Torpedo marmorata*. *FEBS Fed. Eur. Biochem. Soc. Lett.* 33:109–113.
12. Cohen, S. A., and Pumplin, D. W. 1979. Clusters of intramembrane particles associated with binding sites for α-bungarotoxin in cultured chick myotubes. *J. Cell Biol.* 82:494–516.
13. Diamond, J., and R. Miledi. 1962. A study of foetal and newborn rat muscle fibres. *J. Physiol. (Lond.).* 162:393–408.
14. Dryer, F., and K. Peper. 1974. Iontophoretic application of acetylcholine: advantages of high resistance micropipette in connection with an electronic pump. *Pfluegers Arch. Eur. J. Physiol.* 348:362–272.
15. Fambrough, D. M. 1979. Control of acetylcholine receptors in skeletal muscle. *Physiol. Rev.* 59:165–227.
16. Fambrough, D., and J. E. Rash. 1971. Development of acetylcholine sensitivity during myogenesis. *Dev. Biol.* 26:55–68.
17. Fischbach, G. D., and S. A. Cohen. 1973. The distribution of acetylcholine sensitivity over uninnervated muscle fibers grown in cell culture. *Dev. Biol.* 31:147–162.
18. Frank, E., and G. D. Fischbach. 1979. Early events in neuromuscular junction formation in vivo. Induction of acetylcholine receptor clusters in the postsynaptic membrane and morphology of newly formed synapses. *J. Cell Biol.* 83:143–158.
19. Gruener, R., and Y. Kidokoro. 1982. Acetylcholine sensitivity of innervated and non-innervated *Xenopus* muscle cells in culture. *Dev. Biol.* 91:86–92.
20. Hamilton, L. 1969. The formation of somites in *Xenopus*. *J. Embryol. Exp. Morphol.* 22:253–264.
21. Hartzell, M. C., and D. M. Fambrough. 1973. Acetylcholine receptor production and incorporation into membrane of developing muscle fibers. *Dev. Biol.* 30:153–165.
22. Heuser, J. E., T. S. Reese, and D. M. D. Landis. 1974. Functional changes in frog neuromuscular junctions studied with freeze-fracture. *J. Neurocytol.* 3:109–131.
23. Heuser, J. E., and S. R. Salpeter. 1979. Organization of acetylcholine receptors in quick-frozen, deep-etched, and rotary-replaced *Torpedo* postsynaptic membrane. *J. Cell Biol.* 82:150–173.
24. Hirokawa, N., and J. E. Heuser. 1982. Internal and external differentiations of the postsynaptic membrane at the neuromuscular junction. *J. Neurocytol.* 11:487–510.
25. Ito, M. 1960. New electric device for stimulating and recording potentials for single spinal ganglion cells. *In* Medical Electronics. C. N. Smyth, editor. Iliffe, London. 84–85.
26. Kano, M., and Y. Shimada. 1971. Innervation and acetylcholine sensitivity of skeletal muscle cells differentiated *in vitro* from chick embryo. *J. Cell. Physiol.* 78:233–242.
27. Kidokoro, Y., M. J. Anderson, and R. Gruener. 1980. Changes in synaptic potential properties during acetylcholine receptor accumulation and neurospecific interactions in *Xenopus* nerve-muscle cell culture. *Dev. Biol.* 78:464–483.
28. Kidokoro, Y., and R. Gruener. 1982. Distribution and density of α-bungarotoxin binding sites on innervated and non-innervated *Xenopus* muscle cells in culture. *Dev. Biol.* 91:78–85.
29. Kidokoro, Y., S. Heinemann, D. Schubert, B. L. Brandt, and F. G. Klier. 1976. Synapse formation and neurotrophic effects on muscle cell lines. *Cold Spring Harbor Symp. Quant. Biol.* 40:373–388.
30. Kuffler, S. W., and D. Yoshikami. 1975. The distribution of acetylcholine sensitivity at the postsynaptic membrane of vertebrate skeletal twitch muscles: iontophoretic mapping in the micron range. *J. Physiol. (Lond.).* 244:703–730.
31. Kullberg, R. W., T. L. Lentz, and M. W. Cohen. 1977. Development of the myotomal neuromuscular junction in *Xenopus laevis*: an electrophysiological and fine-structural study. *Dev. Biol.* 60:101–129.
32. Land, B. R., T. R. Podleski, E. E. Salpeter, and M. M. Salpeter. 1977. Acetylcholine receptor distribution on myotubes in culture correlated to acetylcholine sensitivity. *J. Physiol. (Lond.).* 269:155–176.
33. Land, B. R., E. E. Salpeter, and M. M. Salpeter. 1980. Acetylcholine receptor site density affects the rising phase of miniature endplate currents. *Proc. Natl. Acad. Sci. USA.* 77:3736–3740.
34. Letinsky, M. S. 1975. Acetylcholine sensitivity changes in tadpole tail muscle fibers innervated by developing motor neurons. *J. Neurobiol.* 6:609–617.
35. Lewis P. R., and A. F. W. Hughes. 1960. Patterns of myoneural junctions and cholinesterase activity in the muscle of tadpoles of *Xenopus laevis*. *Q. J. Microsc. Sci.* 101:55–67.
36. Linstrom, J., S. Tzartos, and W. Gullick. 1981. Structure and function of the acetylcholine receptor molecule studied using monoclonal antibodies. *Ann. N. Y. Acad. Sci.* 377:1–19.
37. Loring, R. H., and H. M. Salpeter. 1980. Denervation increases turnover rate of junctional acetylcholine receptors. *Proc. Natl. Acad. Sci. USA.* 77:2293–2297.
38. Moody-Corbett, F., and M. W. Cohen. 1979. Development of synaptic specializations on cultured, non-innervated, muscle cells at sites of contact with the culture dish. *Soc. Neurosci. Abstr.* 5:486.
39. Moody-Corbett, F., and M. W. Cohen. 1981. Localization of cholinesterase at sites at high acetylcholine receptor density on embryonic amphibian muscle cells cultured withouf nerve. *J. Neurosci.* 1:596–605.
40. Nickel, E., and L. T. Potter. 1973. Ultrastructure of isolated membranes of *Torpedo* electric tissue. *Brain Res.* 57:508–517.
41. Nieuwkoop, P. D., and J. Faber. 1967. Normal Table of *Xenopus Laevis* (Daudin). North-Holland Publishing Co., Amsterdam.
42. Ohmori, H., and S. Sasaki. 1977. Development of neuromuscular transmission in a larval tunicate. *J. Physiol. (Lond.).* 269:221–254.
43. Peng, H. B., and Y. Nakajima. 1978. Membrane particle aggregates in innervated and non-innervated cultures of *Xenopus* embryonic muscle cells. *Proc. Natl. Acad. Sci. USA.* 75:500–504.
44. Peng, H. B., Y. Nakajima, and P. C. Bridgman. 1980. Development of the postsynaptic membrane in *Xenopus* neuromuscular cultures observed by freeze-fracture and thin-section electron microscopy. *Brain Res.* 196:11–31.
45. Paper, K., F. Dreyer, C. Sandri, K. Akert, and H. Moor. 1974. Structure and ultrastructure of the frog motor endplate. *Cell Tissue Res.* 149:437–455.
46. Pumplin, D. W., and D. B. Drachman. 1983. Myasthemic patients' IgG causes redistribution of acetylcholine receptors: Freeze-fracture studies. *J. Neurosci.* 3:576–584.
47. Rash, J. E., C. S. Hudson, and M. H. Ellisman. 1978. Ultrastructure of acetylcholine receptors at the mammalian neuromuscular junction. *In* Cell Membrane Receptors for Drugs and Hormones: a Multidisciplinary Approach. R. W. Straub and L. Bolis, editors. Raven, New York. 47–68.
48. Steinbach, J. H., A. J. Harris, J. Patrick, D. Schubert, and S. Heinemann. 1973. Nerve-muscle interaction in vitro: role of acetylcholine. *J. Gen. Physiol.* 62:255–270.
49. Sytokowski, A. J., Z. Vogel, and M W. Nirenberg. 1973. Development of acetylcholine receptor clusters on cultured muscle cells. *Proc. Natl. Acad. Sci. USA.* 70:270–274.
50. Takahashi, K. 1965. Slow and fast groups of pyramidal tract cells and their respective membrane properties. *J. Neurophysiol.* 28:908–924.
51. Tao-Cheng, J.-H., and J. Rosenbluth. 1980. Nodal and paranodal membrane structure in complementary freeze-fracture replicas of amphibian peripheral nerves. *Brain Res.* 199:249–265.
52. Vogel, Z., A. J. Sytkowski, and M. W. Nirenberg. 1972. Acetylcholine receptor of muscle grown *in vitro*. *Proc. Natl. Acad. Sci. USA.* 69:3180–3184.
53. Yee, A. G., G. D. Fischbach, and M. Karnovsky. 1978. Clusters of intramembrane particles on cultured myotubes at sites that are highly sensitive to acetylcholine. *Proc. Natl. Acad. Sci. USA.* 75:3004–3008.